Investigating the Putative Glycine Hinge in *Shaker* Potassium Channel

Shinghua Ding, Lindsey Ingleby, Christopher A. Ahern, and Richard Horn

Department of Physiology, Institute of Hyperexcitability, Jefferson Medical College, Philadelphia, PA 19107

The crystal structure of an open potassium channel reveals a kink in the inner helix that lines the pore (Jiang, Y.X., A. Lee, J.Y. Chen, M. Cadene, B.T. Chait, and R. MacKinnon. 2002. *Nature* 417:523–526). The putative hinge point is a highly conserved glycine residue. We examined the role of the homologous residue (Gly466) in the S6 transmembrane segment of *Shaker* potassium channels. The nonfunctional alanine mutant G466A will assemble, albeit poorly, with wild-type (WT) subunits, suppressing functional expression. To test if this glycine residue is critical for activation gating, we did a glycine scan along the S6 segment in the background of G466A. Although all of these double mutants lack the higher-level glycosylation that is characteristic of mature *Shaker* channels, one (G466A/V467G) is able to generate voltage-dependent potassium current. Surface biotinylation shows that functional and nonfunctional constructs containing G466A express at comparable levels in the plasma membrane. Compared with WT channels, the shifted-glycine mutant has impairments in voltage-dependent channel opening, including a right-shifted activation curve and a decreased rate of activation. The double mutant has relatively normal open-channel properties, except for a decreased affinity for intracellular blockers, a consequence of the loss of the side chain of Val467. Control experiments with the double mutants M440A/G466A and G466A/V467A suggest that the flexibility provided by Gly466 is more important for channel function than its small size. Our results support roles for Gly466 both in biogenesis of the channel and as a hinge in activation gating.

The Journal of General Physiology

INTRODUCTION

Ion channels are transmembrane proteins that act as conduits for permeant ions to cross the unpropitious hydrophobic environment of the lipid bilayer membrane. Ordinarily the flux of ions is tightly regulated to maintain proper ionic and osmotic gradients across the plasma membrane. This is the job of gates that permit or deny access of ions to the hydrophilic permeation pathway. In voltage-gated ion channels, the gates open and close this pathway in response to changes of membrane potential. However, even in this restricted class of cation-selective ion channels the gates use a variety of conformational processes to open and close the pore. For example, a gate may diffuse into and plug the pore. This occurs during N-type inactivation of voltage-gated potassium (Kv) channels, when the open pore becomes occluded by a tethered cytoplasmic "ball" (Hoshi et al., 1990; Zagotta et al., 1990; Zhou et al., 2001a). Closure of the pore may also be caused by collapse of the region that confers selectivity to specific ions. This has been proposed to occur during the process of slow inactivation of Kv channels (Starkus et al., 1997; Kiss and Korn, 1998; Yellen, 1998, 2002; Kiss et al., 1999). Finally, the activation gate, which is usually the first gate to respond to membrane depolarization, opens as a result of the widening of a four-helix bundle at the cytoplasmic end of the pore (Del Camino et al., 2000; Del Camino and Yellen, 2001; Hackos et al., 2002; Kitaguchi et al., 2004). This bundle consists of the four S6 segments, one from each subunit, that line the cytoplasmic half of the pore, converging to form the activation gate.

The structural changes underlying the opening and closing of the activation gate of potassium channels are unknown, although a variety of alternatives have been proposed for members of this superfamily of ion channels. In several of the early proposals, the four helices approximately maintain their α-helical secondary structure throughout. Opening occurs when these helices pivot away from the symmetry axis of the pore while rotating around their helical axes (Perozo et al., 1999; Flynn and Zagotta, 2001; Johnson and Zagotta, 2001; Liu et al., 2001). The pivot point in this model is near the extracellular end of the S6 segment. In another proposal the activation gate opens by formation of a kink, or "gating hinge," in the middle of the S6 helix (Jiang et al., 2002b; Kelly and Gross, 2003; Tikhonov and Zhorov, 2004; Zhao et al., 2004; Domene et al., 2005). This model is supported by differences in the crystal structures of the homologous helices of closed (Doyle et al., 1998; Kuo et al., 2003) and open (Jiang et al., 2002a,b, 2003) potassium channels, and also by state-dependent cysteine labeling of residues near the bundle crossing of the KcsA potassium channel (Kelly and Gross, 2003). A kink in the inner helix of MthK

Correspondence to Richard Horn: Richard.Horn@jefferson.edu

S. Ding's present address is Department of Neurosciences, University of Pennsylvania School of Medicine, 422 Johnson Pavilion, Philadelphia, PA 19104.

Abbreviations used in this paper: ERK, early response kinase; TBA, tetrabutylammonium; TPentA, tetrapentylammonium; WT, wild-type.

potassium channels (Jiang et al., 2002b) creates an opening wide enough to accommodate intracellular pore blockers as large as tetrabutylammonium (TBA, ~12 Å in diameter). In spite of its large size, TBA can enter deeply into a potassium channel when it is open (Zhou et al., 2001a). The 30° kink observed in the MthK structure occurs near a glycine (Gly) residue that is highly conserved in the pore-lining helices of many potassium channels, whether or not they are gated by voltage (Jiang et al., 2002b). Gly residues are known to confer flexibility to protein structures (Li and Deber, 1992; Bright and Sansom, 2003), making them excellent candidates to act as movable hinges. In a final proposal, a variant of hinged opening, a proline-based kink below the conserved Gly in S6 segments exists in both open and closed channels and somehow contributes to the gating of Kv channels (Holmgren et al., 1998; Del Camino et al., 2000; Del Camino and Yellen, 2001; Labro et al., 2003; Webster et al., 2004). The role of the upstream Gly in this proposal is unclear.

Here we examine the idea of a Gly hinge by showing first that alanine, the amino acid residue that maximally stabilizes α-helices (O'Neil and DeGrado, 1990; Chakrabartty et al., 1991), cannot substitute for Gly466 in the S6 segment of *Shaker* potassium channels. Tetramers that include even one G466A subunit are nonfunctional. We further test whether a Gly residue, substituted elsewhere along the S6 segment, can restore voltage-dependent gating to the nonfunctional G466A mutant. Our Gly scan uncovered only one functional double mutant, G466A/V467G, which had alterations in activation gating. Besides these results that support the idea that a Gly hinge is used during voltage-dependent opening of the activation gate, we also found that any construct containing the G466A mutation lacked the typical high molecular weight glycosylation feature of wild-type (WT) *Shaker*, suggesting a further role of this Gly residue in biogenesis of potassium channels.

MATERIALS AND METHODS

Mutagenesis and Expression

Mutations were generated by PCR as previously described (Ding and Horn, 2002). The WT background we used was *Shaker* H4 with the following four modifications: deletion of residues 6–46 to remove N-type inactivation, T449V to inhibit C-type inactivation, and C301S and C308S. All mutations were verified by sequencing, and many of the constructs were epitope tagged with FLAG (DYKDDDDK) inserted into either the COOH terminus (pBSTA vector; gift of A.L. Goldin, University of California, Irvine, CA) or the NH_2 terminus (pGW1-CMV vector; British Biotechnology). Both mammalian cells (tsA201 and HEK293) and *Xenopus* oocytes were used for expression. Mammalian cells were transiently transfected with a standard calcium phosphate method. *Xenopus* oocytes were injected with cRNA prepared by in vitro transcription. The oocytes were then maintained at 19°C for 2–3 d until used for recording. In studies of dominant-negative suppression (e.g., Fig. 1 B) we verified that expression of WT channels was not affected in a nonspecific manner by coinjecting oocytes with pHook-1 (Invitrogen) cRNA at a molar level 20-fold higher than the *Shaker* subunit. pHook-1 is a single transmembrane protein with a myc tag at its NH_2 terminus. We verified pHook-1 expression in these experiments by Western blot using an antibody against myc (not depicted). pHook-1 had insignificant effects on the levels of WT currents in five separate experiments.

Biochemistry

HEK 293 cells (60% confluence) were transfected with 20 mg WT or mutant DNA and cultured for 48 h. Cells were homogenized in lysis buffer (20 mM Na_2HPO_4, 30 mM $Na_4P_20_7$, 1 mM $MgCl_2$, 0.5 mM EDTA, 300 mM sucrose, protease inhibitor cocktail [Roche], pH ~9.3), and centrifuged at 500 *g* for 5 min. The supernatant was centrifuged at 50,000 *g* for 30 min and the pelleted membrane fraction resuspended in lysis buffer. Protein concentration was determined using the Bradford Assay (Bio-Rad Laboratories). Samples (equal protein) were separated by SDS-PAGE and transferred to PVDF membrane (Millipore). Immunoblots were blocked with 5% milk, 0.1% Tween-20 in Tris-buffered saline, pH 7.5, and probed sequentially with anti-FLAG (Stratagene) antibody and secondary HRP-conjugated antibody (Roche) diluted in blocking solution. Detection was by enhanced chemiluminescence (PerkinElmer). Surface expression of *Shaker* mutants in transfected cells was assayed by the "Cell Surface Protein Biotinylation and Purification Kit" (Pierce Biotechnology). For biotinylation experiments we used the cytoplasmic protein early response kinase (ERK) as a negative control. ERK was detected by an anti-ERK antibody (Promega).

Electrophysiology

Whole cell currents from transfected cells were obtained as described previously (Ding and Horn, 2003). For whole cell recording, the patch pipette contained (in mM) 105 CsF, 35 NaCl, 10 EGTA, 10 Hepes, pH 7.4. The bath contained (in mM) 150 NaCl, 2 KCl, 1.5 $CaCl_2$, 1 $MgCl_2$, 10 Hepes, pH 7.4. For analysis of selectivity we used either whole cell currents or outside-out patches in which all of the intracellular Cs^+ was replaced with Rb^+, and the extracellular Na^+ and K^+ were completely replaced with either Rb^+ or K^+. Whole cell currents from oocytes were obtained by standard two-microelectrode voltage clamp using a bath of (in mM) 116 NaCl, 2 KCl, 2 $MgCl_2$, 1.8 mM $CaCl_2$, 5 Hepes, pH 7.6.

Experiments examining single channels or nonstationary noise analysis used cell-attached patches from oocytes. In these studies the pipette solution contained (in mM) 140 NaCl, 10 KCl, 5 $MgCl_2$, 10 Hepes, pH 7.2. Block by tetraalkylammonium cations was studied with inside-out patches using the same pipette solution, and a bath containing (in mM) 140 KCl, 2 $MgCl_2$, 1 $CaCl_2$, 11 EGTA, 10 Hepes, pH 7.2.

Data Analysis

Data were analyzed using pCLAMP (Axon Instruments), ORIGIN 7.5 (OriginLab), and Fortran (Compaq). Selectivity of Rb^+ over K^+ was estimated from shifts in reversal potential ΔV_{rev} under biionic conditions (Fig. 5) according to

$$\frac{P_{Rb^+}}{P_{K^+}} = \exp\left(\frac{\Delta V_{rev} F}{RT}\right),$$

where $RT/F = 25$ mV at room temperature. Nonstationary noise analysis used previously described methods (Ding and Horn, 2002). Throughout the paper, error bars represent the standard error of the mean.

Block

Block by intracellular TBA and tetrapentylammonium (TPentA) were studied in inside-out oocyte patches. K_d, the dissociation

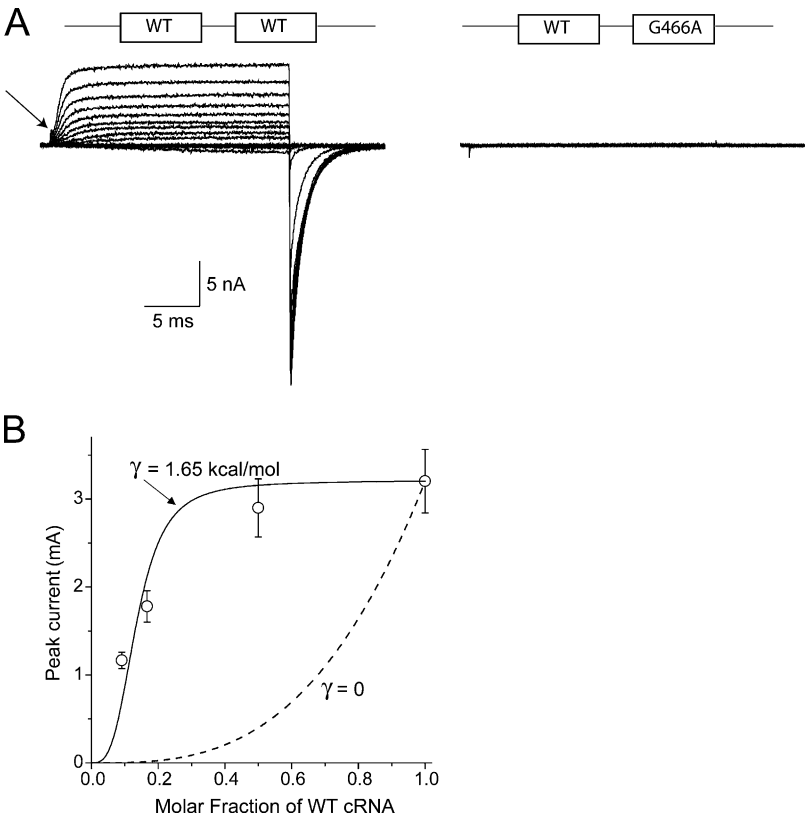

Figure 1. Wild-type subunits cannot rescue the lethality of the G466A subunits. (A) Whole cell Cs^+ currents in tandem dimers. Holding potential, −120 mV, depolarizations from −80 to +60 mV in 10-mV increments. WT-WT tandem produces currents comparable to those of WT monomers. The arrow shows gating current. A tandem dimer of WT and G466A, with the mutant downstream of the WT, is completely nonfunctional. Cotransfected tsA201 cells were identified by 4-μm beads coated with CD8 antibody (Dynal Biotech). The tandem construct included the extra linker residues -NNNNNNAMN- between the two protomers. (B) Dominant-negative suppression. Coexpression of WT and G466A monomers reduces peak WT current amplitude at +70 mV in oocytes (n = 15–18 oocytes for each data point). The same molar amount of cRNA for WT was injected in each condition, with the remaining volume adjusted appropriately with water or mutant cRNA. The abscissa represents the molar fraction of WT cRNA. The dashed line is the suppression predicted by the binomial equation. The solid line is a single-parameter fit of a model in which there is an assembly penalty of 1.65 ± 0.14 kcal/mol for each mutant–WT contact in a tetramer (APPENDIX).

constant for block, was estimated from the dose–response relationship at +80 mV, using the relationship $K_d = [B]F_{un}/(1 - F_{un})$, where the blocker concentration is [B] and F_{un} is the steady-state fraction of unblocked current. Note that this relationship ignores possible effects of open probability on block (see Ding and Horn, 2002). If all of the steady-state channel gating observed at membrane potentials >+20 mV is due to movement of the activation gate, K_d could be overestimated by at most ∼30% by ignoring open probability, because peak open probability estimated by nonstationary noise analysis was typically >0.7. The kinetics of block were determined from WT patches using the time course of current reduction during a depolarizing voltage step. The concentration-dependent blocking rate ρ is the inverse of the single-exponential time constant of block. The association rate constant for a one-step blocking reaction is estimated as $k_{on} = \rho/(K_d + [B])$, and the dissociation rate constant is $k_{off} = \rho F_{un}$. The blocking rate ρ for the G466A/V467G mutant was determined by stationary noise analysis (Neher and Stevens, 1977). Currents were obtained in inside-out patches in response to ∼160 depolarizations to +80 mV. Currents were lowpass filtered at 20 kHz and sampled at 200 kHz. Power spectra were calculated for each depolarization, using a discrete Fourier transform implemented in Fortran, and averaged. Resultant spectra were fit by a sum of 1/f noise and a lorentzian component with a corner frequency f_c. The blocking rate was estimated as $\rho = 2\pi f_c$ (Baukrowitz and Yellen, 1996), and the association and dissociation rate constants were determined as above.

RESULTS

The G466A mutant in *Shaker's* S6 segment is nonfunctional (Yifrach and MacKinnon, 2002; Magidovich and Yifrach, 2004), supporting the hypothesis that the flexibility bestowed by Gly466 is important for the activation gate to open. The lethality of this mutation in a homotetrameric channel raises the question whether a functional channel could be formed in a heterotetramer of WT and mutant (Gly466A) subunits. This might be expected, based on the fact that in eukaryotic voltage-dependent sodium channels, one of the four S6 segments (D4/S6) is missing this conserved Gly residue. Initially we tested whether WT *Shaker* subunits could rescue mutant subunits by constructing tandem dimers in which either both subunits were WT, or else one had the G466A mutation. Only the former tandem construct was functional in mammalian cells (Fig. 1 A). The G466A mutant not only lacks ionic current, but also the gating current that usually precedes opening of the activation gate (arrow in Fig. 1 A; e.g., Ding and Horn, 2003). In voltage-gated ion channels this gating current is due to the movement of the channel's voltage sensors, primarily the positively charged S4 segments, in response to a step depolarization. It is unlikely that the immobility of the voltage sensor is due to inflexibility of the S6 segment, we believe, because in WT channels most of this charge movement occurs before the activation gate opens (Bezanilla, 2000). Moreover, other S6 mutations are capable of abolishing ionic current while leaving gating currents relatively intact (Hackos et al., 2002; Kitaguchi et al., 2004). This raises the possibility that the G466A mutation affects biogene-

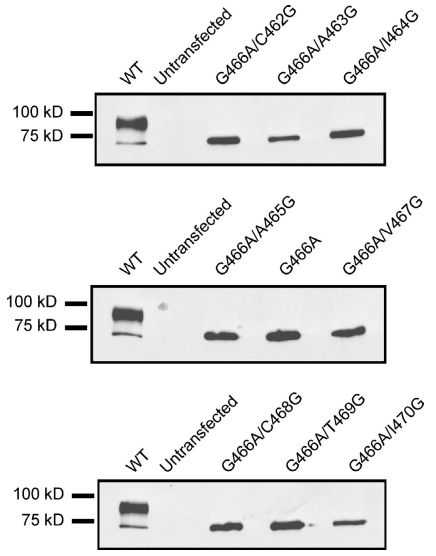

Figure 2. Western blots show that all constructs containing G466A, including the functional mutant G466A/V467G, produce roughly comparable amounts of protein, but with restricted glycosylation, as shown by the absence of the high molecular weight band observed in the WT.

sis or transport to the plasma membrane, an issue we address below. Note that the perniciousness of the G466A mutation contrasts with the innocuous effects of alanine substitutions of homologous Gly residues in two of the S6 segments of a voltage-dependent sodium channel (Yarov-Yarovoy et al., 2002), suggesting the possibility of significant differences in activation gate opening in these two related classes of ion channels.

To test the ability of G446A subunits to participate in heterotetramer formation with WT channels, we coexpressed WT and G466A monomers both in mammalian cells and in *Xenopus* oocytes. The biophysical properties of the resultant currents were indistinguishable from those of WT channels (not depicted), except that the currents were reduced in amplitude (Fig. 1 B), indicative of a dominant-negative suppression. Note that the amplitudes of WT control currents were unaffected by coexpressing a 20-fold higher molar equivalent of the transmembrane protein pHook-1, ruling out nonspecific effects of cRNA injection (MATERIALS AND METHODS). These data suggest that mutant subunits can coassemble with WT subunits, and that even a single mutant subunit within a tetramer destroys function.

The dashed line in Fig. 1 B shows the relationship predicted by the binomial distribution (see APPENDIX) between the potassium current amplitude and the fraction p of WT cRNA injected into the oocytes. The suppression observed experimentally is grossly overestimated by this theoretical prediction. Two immediate explanations come to mind. The first is that p is much larger than we believe under the conditions of our experiments. Quantitatively the results in Fig. 1 B can be fit reasonably well

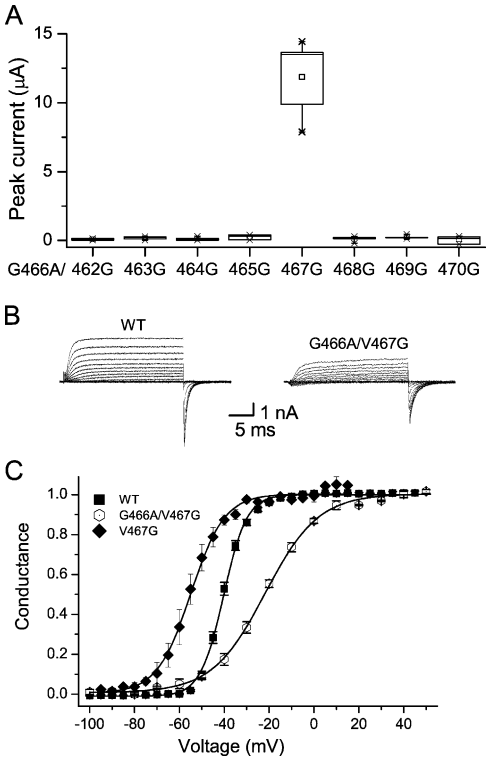

Figure 3. Functionality tested in Gly mutants. (A) Functional Gly scan using FLAG-tagged double mutants expressed in *Xenopus* oocytes. Peak currents at +50 mV. All mutants contained G466A and cRNAs were injected at equimolar concentrations. Recordings were obtained 2 d after injection, n = 3–6 eggs. Similar results were obtained for all double mutants using mammalian cell expression (not depicted). (B) Cs^+ currents obtained in whole cell recording as described in Fig. 1 A. (C) *G-V* relationships for Cs^+ currents in WT, V467G, and G466A/V467G constructs (n = 4 in each case) in mammalian cells. These relationships were determined from isochronal tail current measurements. The *G-V* relations were fitted to the Boltzmann equation:

$$G(V) = \frac{1}{1 + \exp[-qF(V - V_{1/2})/RT]},$$

where $G(V)$ is normalized conductance, $V_{1/2}$ is the half activation voltage, q is the unitless slope, and RT/F is 25 mV at room temperature. For WT: $V_{1/2}$, q was −40.5 ± 0.8 mV, 4.99 ± 0.13; for V467G: $V_{1/2}$, q was −55.2 ± 2.4 mV, 3.50 ± 0.23; for G466A/V467G: $V_{1/2}$, q was −22.0 ± 1.2 mV, 2.16 ± 0.11. Free energy differences were calculated as $\Delta\Delta G = \Delta(qFV_{1/2})$ for any two constructs. Although this is only a crude measure of the open–closed equilibrium energy, an improved approach based on the assumption that S6 mutants affect only the concerted opening transition (Yifrach and MacKinnon, 2002) is inconsistent with the differences between WT and the V467G mutant, because the mutation causes the *G-V* relationship to be both left shifted and shallower than that of the WT.

if WT protein expresses ~12-fold better than mutant protein (calculations not shown). We reject this possibility, however, because it is inconsistent with our biochemical data (Fig. 2) that show very similar expression levels of mutant and WT protein. Moreover, the presence of comparable levels of mutant and WT protein on the cell surface (Fig. 4) suggests that mutant subunits form ho-

motetramers approximately as well as WT subunits. The second possibility is that homotetramers, of either WT or mutant subunits, assemble more readily than the heteromers that produce suppression. The solid line in Fig. 1 B is the prediction of a model in which each mutant: WT contact within a tetramer carries a fixed penalty of 1.65 ± 0.14 kcal/mol for assembly (see APPENDIX). Although this is only one of several possible explanations for the impoverished suppression in these experiments, it adequately accounts for the data.

Glycine Scan

We tested the proposal that a hinge is necessary for channel opening by performing a glycine scan in the background of the nonfunctional G466A mutant. Eight double mutants were examined, four above and four below G466A. All FLAG-tagged mutants express protein (Fig. 2). None, however, is as extensively glycosylated as WT channels, as evidenced by the absence in the mutants of a higher molecular weight band characteristic of a mature form of the channel (Santacruz-Toloza et al., 1994; De Souza and Simon, 2002). The lower weight band typically represents immature channels that are only core glycosylated, and may be retained in the endoplasmic reticulum (Santacruz-Toloza et al., 1994; Papazian et al., 1995; De Souza and Simon, 2002). This is not an absolute impediment to surface expression, however, because mutations that remove the glycosylated asparagine residues of *Shaker* do not obliterate potassium currents (Santacruz-Toloza et al., 1994). Indeed, one of the double mutants, G466A/V467G, is functional (Fig. 3, A and B), indicating that a substantial fraction of the protein escaped the endoplasmic reticulum to reach the plasma membrane.

The ability of G466A/V467G alone to yield potassium currents has two possible explanations. V467G could either rescue function or reestablish trafficking to the plasma membrane. To discriminate these two alternatives we compared surface expression of three FLAG-tagged constructs, WT, G466A, and G466A/V467G, using a biotinylation assay. Surface proteins were indiscriminately labeled with a membrane-impermeant bifunctional reagent that covalently attaches biotin to primary amines. These surface proteins were immunoprecipitated with neutravidin and probed with FLAG antibody. Fig. 4 shows a similar pattern of staining for whole cell lysates (left) and immunoprecipitated protein (right) from the same transfected cells, indicating that functional (WT and G466A/V467G) and nonfunctional (G466A) channels are all expressed on the cell surface at comparable levels. Control experiments show that an endogenous cytoplasmic protein (ERK) is not immunoprecipitated under the same conditions (Fig. 4). Our results indicate that V467G rescues function, rather than trafficking to the cell surface. Nevertheless,

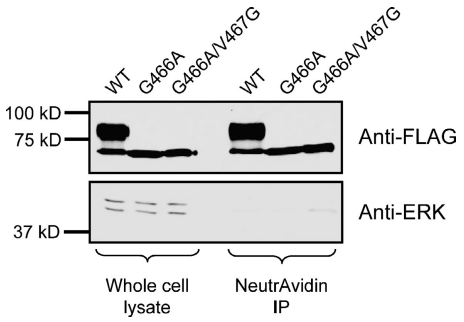

Figure 4. Constructs containing G466A, whether functional or not, are expressed on the plasma membrane. The top/bottom panel is blotted with anti-FLAG/anti-ERK antibody, respectively. The left side is protein from whole cell lysates of tsA201 cells transfected with the indicated constructs (see Fig. 2) and immunoprecipitated surface protein from the same cells on the right. The FLAG western shows comparable expression levels for the three *Shaker* constructs, both in whole cell lysates and from surface protein. Western blots from the same material shows the presence of the cytoplasmic proteins ERK1 (top band) and ERK2 in whole cell lysates but not from surface protein.

the amplitudes of WT currents, both in mammalian cells and in *Xenopus* oocytes, are typically ~5–10-fold larger than obtained with G466A/V467G channels (unpublished data). The cause of this difference in current amplitude is not evident because, as we show later, individual G466A/V467G channels have a maximum open probability that approaches that of the WT. We interpret these composite results as an indication that G466A produces some defect in biogenesis that inhibits glycosylation, in addition to a destruction of function. Only the functional defect of the G466A mutation is rescued by V467G.

The double mutant G466A/V467G is reluctant to open. The depolarizing shift in the conductance–voltage (*G-V*) relationship, decrease in its slope (Fig. 3 C), and slowing of activation kinetics (Fig. 5 A) all suggest that the mutations shift the equilibrium of the final opening transition in the activation pathway away from the open state, as described for some other mutations along the S6 segment (Yifrach and MacKinnon, 2002). Energetically this double mutation increases the work of opening the channel by $\Delta\Delta G = 3.56$ kcal/mol (see legend of Fig. 3). To examine the energetic effect of G466A alone, we compared the *G-V* relationship of the single mutant V467G with that of G466A/V467G. The *G-V* curve of the single mutant is left shifted and steeper than that of the double mutant (Fig. 3 C); the energetic consequence of introducing G466A on the background of V467G is equivalent to $\Delta\Delta G = 3.36$ kcal/mol. If mutations of these adjacent residues are assumed to have independent consequences on activation gating, the single mutation V467G is energetically rather insignificant (<0.4 kcal/mol) compared with the effect of mutating residue Gly466.

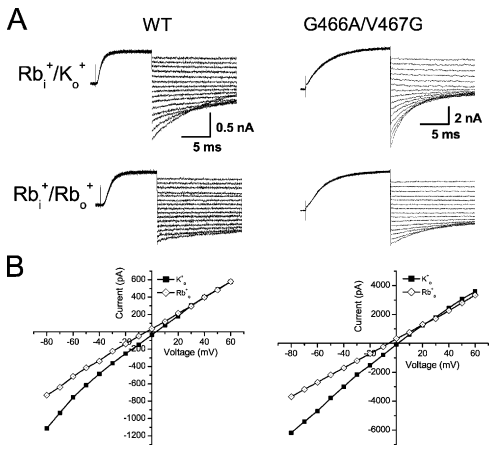

Figure 5. The G466A/V467G mutations have no effect on Rb^+/K^+ selectivity. (A) Currents shown from either an outside-out patch (WT on left) or whole cell recording (G466A/V467G on the right). Voltage protocols described in the text. (B) Reversal potentials of isochronal I-V plots were obtained by linear interpolation. Rb^+ solutions caused a -6.9 ± 0.7 mV shift in WT ($n = 4$ cells) and a -4.7 ± 0.9 mV shift in mutant ($n = 6$) channels.

Open Channel Properties of the G466A/V467G Mutant

We might expect that a displaced gating hinge would affect open channel properties, due either to the proximity of the mutations to the channel's selectivity filter, or to how wide the activation gate is able to open. We explore three of these properties here: selectivity, single channel conductance, and pore block by tetraalkylammoniums.

Fig. 5 shows that the relative permeability of Rb^+ and K^+ ions is unaffected in the double mutant. The WT (left) and mutant (right) panels show currents in the presence of either high extracellular [K^+] (above) or high extracellular [Rb^+] (below). Currents were activated by a depolarization to +75 mV and followed by hyperpolarizing steps to voltages between +60 and −80 mV. Amplitudes of isochronal tail currents are plotted in Fig. 5 B. The leftward shift of reversal potential in a Rb^+ bath indicates that K^+ ions are moderately more permeable than Rb^+ ions. The comparable shift for WT and G466A/V467G channels indicates that the double mutation has little effect on selectivity. The permeability ratios P_{Rb+}/P_{K+} based on these shifts were 0.76 ± 0.02 ($n = 4$) for WT channels and 0.83 ± 0.03 ($n = 6$) for G466A/V467G channels ($P > 0.05$, t test).

Point mutations in the vicinity of the open activation gate are known to affect single channel conductance (Ding and Horn, 2002). This suggests that alterations in S6 conformation in the open state might produce changes in flux of K^+ ions through the channel. To test this, we examined single channel conductance for K^+ in either of two ways, single channel recording (Fig. 6 A) or nonstationary noise analysis (Fig. 6 B). The single channel conductance was marginally larger in the double mutant than in WT patches (see Fig. 6 and legend),

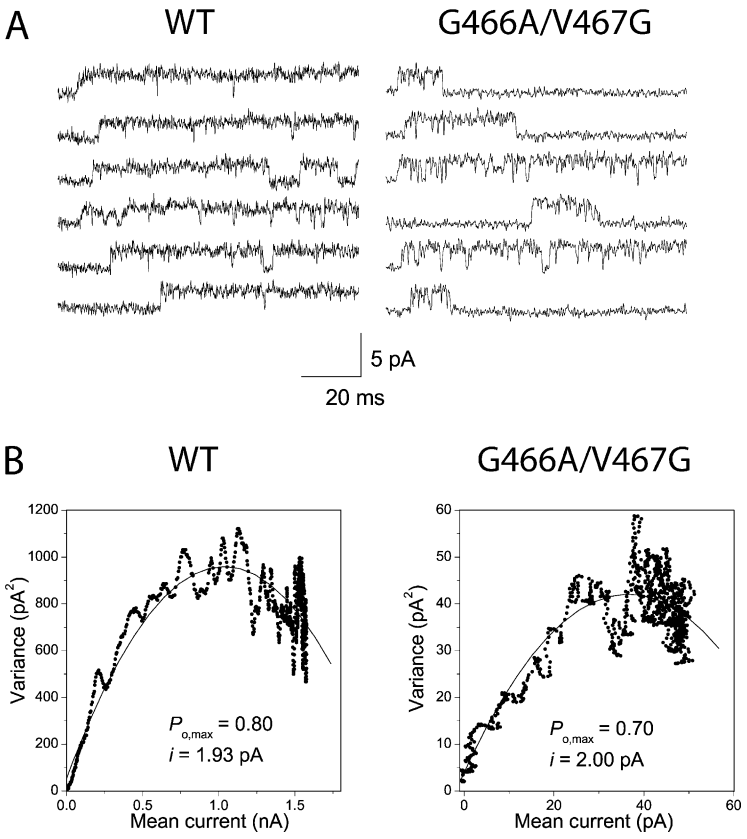

Figure 6. The G466A/V467G mutations have little effect on single channel conductance. (A) Examples of single channel openings in response to steps to +80 mV from a holding potential of −70 mV in cell-attached patches. Low-pass filter, 2 kHz. Data from these two patches were fit by amplitude histograms producing estimates of 2.01 pA for WT and 2.22 pA for G466A/V467G. (B) Nonstationary noise analysis for depolarizations to +80 mV in two cell-attached patches, 10 kHz low-pass filter. Estimates of single channel current i amplitude and $P_{open,max}$ are shown. Estimates of i and $P_{open,max}$ in nine WT patches were 1.84 ± 0.07 pA and 0.78 ± 0.01, respectively. In six G466A/V467G patches the estimates of i and $P_{open,max}$ were 2.30 ± 0.09 pA and 0.68 ± 0.02, respectively.

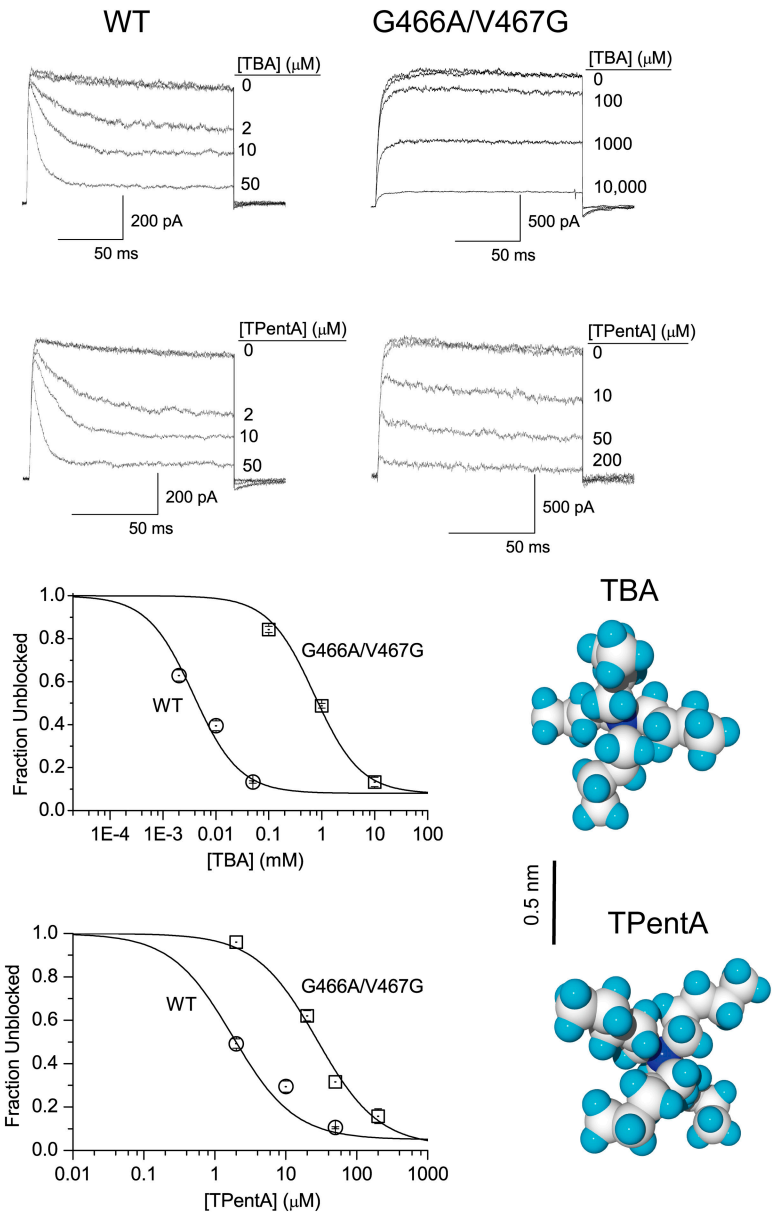

Figure 7. The G466A/V467G mutations reduce block of intracellular tetraalkylammonium cations. Data shown from inside-out patches with reagents at indicated concentrations. Currents at +80 mV before and after exposure to blocker are superimposed. Dose–response relationships are shown in the bottom panels with molecular models of the blockers on the right. Data were fit using a single-site blocking model with K_d values of 3.77 μM (TBA) and 1.72 μM (TPentA) for WT channels, and K_d values of 730 μM (TBA) and 27.6 μM (TPentA) for G466A/V467G (n = 3–5).

suggesting only minor effects on the structure of the open activation gate.

Block

The open MthK channel has an inner mouth that is open just wide enough to accommodate a blocker as large as TBA, ~12 Å in diameter (Zhou et al., 2001a; Jiang et al., 2002b). This opening is apparently a consequence of the kink near the Gly466 homologue in MthK (Jiang et al., 2002b). We ask here whether a shifted Gly hinge opens the activation gate as wide by testing the block of TBA and its larger relative, TPentA (Fig. 7). We examine the block of these two cations using inside-out oocyte patches.

Fig. 7 shows two features of block that differ between mutant and WT channels for currents elicited at +80 mV. First, the block is considerably more potent in WT than in G466A/V467G channels, 190-fold for TBA and 16-fold for TPentA. Second, the blocking kinetics are resolvable for WT, but not for G466A/V467G, channels. There are several possible explanations for these differences; we will dissect them one at a time.

The blocking site for TBA is deep within the permeation pathway in WT channels (Zhou et al., 2001a). Perhaps the decreased potency observed in the double mutant is due to the fact that the open activation gate is not wide enough to permit the blocker to enter, and therefore it might have a more superficial blocking site. We tested this possibility by examining the voltage dependence of block, which largely reflects the displacement of permeant ions by the blocker (Spassova and Lu, 1998). The steady-state fraction of blocked

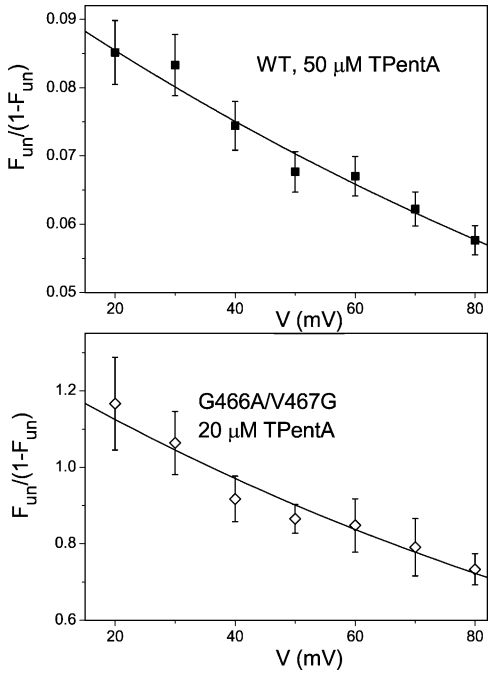

Figure 8. The G466A/V467G mutations have little effect on the voltage dependence of TPentA block. Steady-state block at voltages between +20 and +80 mV from inside-out patch currents as in Fig. 7. The data were fit by the equation $F_{un}/(1 - F_{un}) = C \cdot \exp(-\delta VF/RT)$, where F_{un} is the steady-state fraction of unblocked current, C is a constant, and δ is a unitless parameter representing the fraction of the electric field at the blocking site felt by the blocker and any ions that move with it. The estimates of δ were 0.15 ± 0.01 and 0.18 ± 0.03 for WT and G466A/V467G, respectively, for $n = 3$ patches each. These values are not significantly different ($P > 0.05$, t test).

channels was determined by experiments comparable to those shown in Fig. 7, except that the test potential was varied between +20 and +80 mV. Fig. 8 shows that TPentA block is exponentially dependent on membrane potential, with an insignificant difference ($P > 0.05$, t test) in voltage dependence between WT (δ = 0.15 ± 0.01, $n = 4$) and G466A/V467G (δ = 0.18 ± 0.03, $n = 4$) channels. These data suggest that the blockers reach comparable locations deep within the pore, but that the binding affinity is reduced in the double mutant.

Another factor that could reduce the apparent potency of block is a reduction of maximal open probability, because intracellular tetraalkylammonium cations can only block open channels (Armstrong, 1971). Maximal open probability $P_{open,max}$ was estimated from nonstationary noise analysis (Fig. 6 B). Although $P_{open,max}$ is moderately reduced in the double mutant, by <15%, this cannot account for the dramatic differences in equilibrium block. These results therefore suggest a true difference in affinity of the open channel for TBA block between wild-type and G466A/V467G channels.

If we assume a simple model in which block involves a 1:1 collision between the blocker and its site within the pore, a decreased affinity can be explained by changes in either or both of two rate constants. The double mutant could decrease the second-order blocking constant k_{on} and/or increase the unbinding rate constant k_{off}. Mechanistically, these alternatives lead to very different insights into the effect of the double mutation. A decrease of k_{on} suggests an increase in the activation free energy barrier for the blocker to reach its binding site, whereas an increase of k_{off} implies an increase in the free energy (i.e., destabilization) of the blocker-bound state. Our data tend to support the latter alternative, because the blocking kinetics are only slow enough to resolve in wild-type channels (Fig. 7). The two rate constants underlying block are readily estimated (see MATERIALS AND METHODS) in wild-type channels from the time constant of TBA block (34.2 ± 1.3 ms at +80 mV for 2 mM TBA, $n = 4$) and the dissociation blocking constant K_d (3.40 ± 1.04 μM at +80 mV). This analysis produces estimates for k_{on} and k_{off} of $5.44 \times 10^6\ M^{-1}s^{-1}$ and $18.5\ s^{-1}$, respectively.

Estimation of these two rate constants requires both kinetic and equilibrium measurements. Because TBA blocking kinetics are not readily apparent in macroscopic currents of the G466A/V467G mutant (Fig. 7), we resorted to stationary fluctuations to measure blocking kinetics at frequencies up to 10 kHz. Fig. 9 (A and C) shows the mean and variance of currents from inside-out patches in the absence and presence of 1 mM TBA. The currents were generated from 160 depolarizations to +80 mV. The double arrows indicate the region used for stationary noise analysis. Control spectra in the absence of blocker were always well fit by a 1/f function ($n = 4$) with spectral densities orders of magnitude larger than background fluctuations at the −80 mV holding potential (Fig. 9 B). TBA introduces a lorentzian component with a corner frequency (f_c, arrow) of 2860 Hz (Fig. 9 D). Similar spectra were obtained from four patches in which f_c was 2964 ± 64 Hz. If we assume that this component represents TBA blocking kinetics, and that TBA block is insensitive to the gating transitions responsible for the 1/f noise (Baukrowitz and Yellen, 1996), these data allow us to estimate k_{on} and k_{off} (see MATERIALS AND METHODS) of $10.8 \times 10^6\ M^{-1}s^{-1}$ and $7.83 \times 10^3\ s^{-1}$, respectively. The large value of k_{off} predicts a mean dwell time of only 128 μs for TBA in its blocking site. This would have been extremely difficult to resolve unambiguously with single channel recording.

A comparison of these rate constants between WT and the G466A/V467G mutant shows that almost the entire effect of shifting the putative gating hinge on TBA block is due to a 420-fold increase of k_{off} (3.5 kcal/mol), compared with a twofold change of k_{on} (<0.5

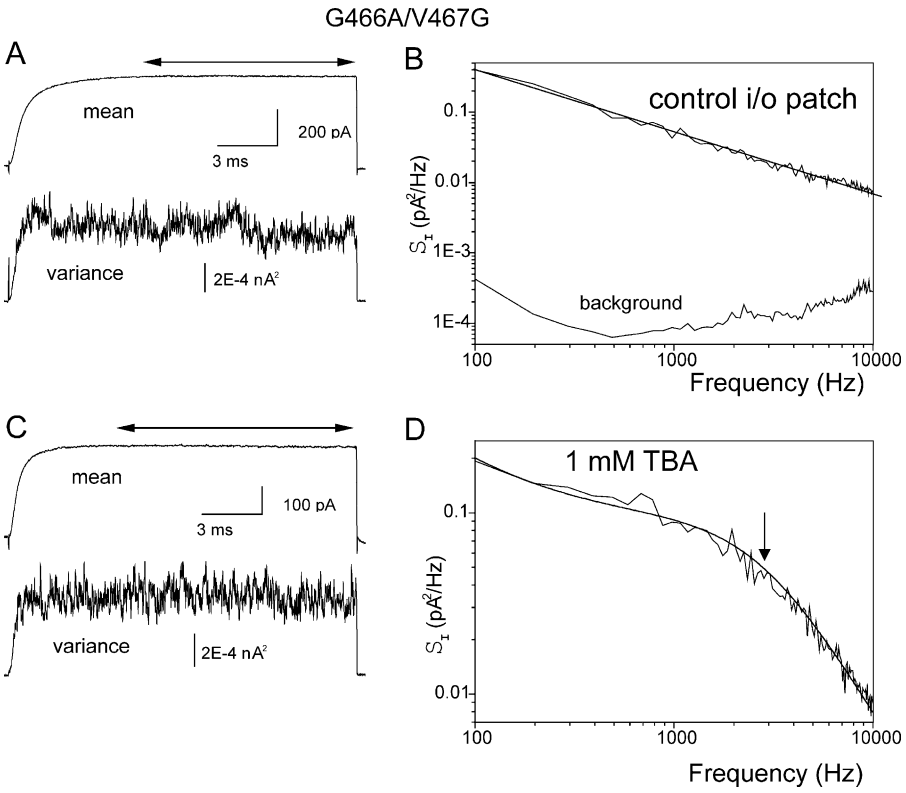

Figure 9. Estimates of TBA blocking constants using stationary noise. Inside-out patches for G466A/V467G mutants in the absence (A and B) and presence (C and D) of 1 mM TBA. 160 depolarizations to +80 mV were applied, and stationary noise was measured over the intervals shown by the double arrows. A and C show mean and variance for these currents, with spectra shown in B and D. The spectrum of background noise at the −80 mV is shown in B. Data were fit by a weighted sum of a lorentzian and 1/f noise. The arrow indicates the corner frequency f_c of the lorentzian in the patch exposed to 1 mM TBA.

kcal/mol). The small effect on k_{on} suggests a minor change in the energy barrier for entry of TBA, implying that the activation gate of the G466A/V467G mutant opens just as wide as in the wild-type channel.

What could account for the large increase of k_{off} in the double mutant? A previous study showed that a mutation in Kv1.4 equivalent to V467A of *Shaker* caused an ~1 kcal/mol destabilization of TBA block (Zhou et al., 2001a). Moreover, crystal structures of potassium channels show that the residues homologous to Val467 extend their side chains into the central permeation pathway (Fig. 10 A). These facts suggest that the decreased potency of TBA block in the G466A/V467G mutant is due more to the loss of the greasy side chain of Val467 than to the G466A mutation. This proposal was confirmed by measuring TBA block of the single mutant V467G, which increased K_d from 3.77 μM to 2.47 ± 0.20 mM (3.8 kcal/mol, $n = 3$), an effect even larger than observed for the double mutant in which K_d was 0.73 mM (Fig. 7). This suggests that the G466A mutation itself modestly stabilizes TBA block.

Our data therefore show little effect of the double mutation G466A/V467G on the biophysical properties, and presumably the conformation, of the open state. Rather, the biophysical consequence of shifting Gly466 downstream by one residue is a disinclination of the channel to enter and remain in the open state, consistent with Gly466 contributing to a gating hinge.

Packing or Flexibility?

A Gly residue has two hallmark properties that are instrumental to its unique roles in a protein. The first, its small size, is known to be important for close packing of α helices, especially in membrane proteins (Lemmon and Engelman, 1994; Javadpour et al., 1999; Russ and Engelman, 2000). The second is its ability to confer flexibility to an α helix (see DISCUSSION). We have interpreted our results largely in terms of the latter property. An alternative possibility, however, is that the G466A mutation abolishes function by disrupting packing, and that the rescue of function by V467G is due not to a restoration of flexibility, but to a compensatory decrease in side-chain volume that partially restores normal packing. In support of this idea a crystallographic study of the KirBac1.1 channel advanced the idea that the Gly residue homologous to Gly466 of *Shaker* is involved mainly in packing and is not acting as a pivot point for gating (Kuo et al., 2003). The main argument against this explanation for V467G's ability to rescue function in the G466A mutant is that the side chain of Val467 appears not to be involved in helical packing (Fig. 10 A). Nevertheless, we tested this possibility by constructing two additional mutations specifically designed to try to rescue the lethal mutation G466A from disruptions of packing.

Based on available crystal structures, the introduced alanine of *Shaker*'s G466A is expected to clash with a hydrophobic residue at the COOH-terminal end of the

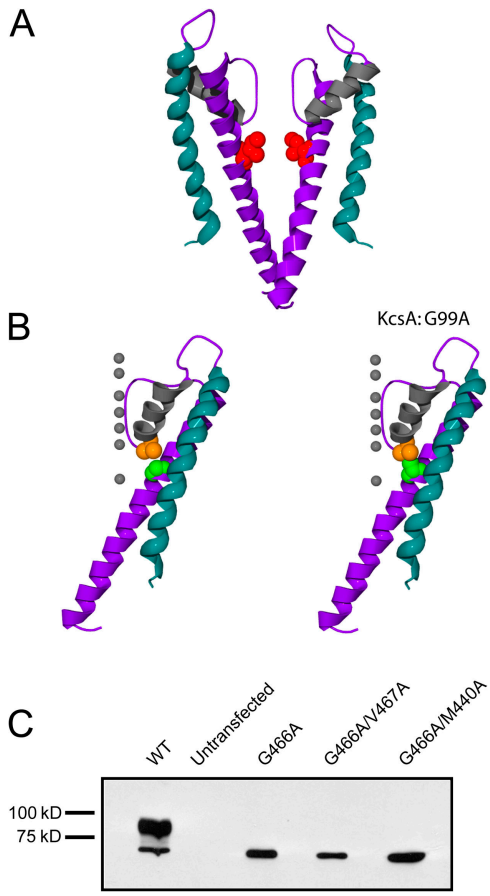

Figure 10. Tests of steric clash. (A) Two opposing subunits of KcsA from a high-resolution crystal structure (1K4C; Zhou et al., 2001b), highlighting the position of the pore-lining residue homologous to Val467 in *Shaker* (red). Drawn with Swiss-PdbViewer (http://us.expasy.org) and POV-Ray (www.povray.org). (B) Single KcsA subunits showing the homologue to *Shaker*'s Met440 (orange) and Gly466 (green) on the left, and the expected clash due to the G466A mutation on the right. K^+ ions are depicted as gray spheres. (C) Western blot as in Fig. 2 showing poor glycosylation of all mutants containing G466A.

pore helix (Ala73 in KcsA, Ile57 in MthK, or Ala194 in KvAP). A high-resolution structure of KcsA (1K4C, 2.00 Å; Zhou et al., 2001b) is shown in Fig. 10 B (left), along with the expected effect of the G99A mutation that introduces this steric clash in KcsA (right). The *Shaker* homologue of Ala73 in KcsA is Met440. The M440A mutation will reduce the volume of this side chain by 57 $Å^3$. By itself this mutation is functional (Yifrach and MacKinnon, 2002). We tested whether M440A could rescue the function of the G466A mutation (a 19-$Å^3$ increase of side-chain volume). The double mutant M440A/G466A was nonfunctional (no voltage-activated currents in 14 transfected cells [our stringent functional test was a step depolarization from −190 to +100 mV]). We saw neither ionic nor gating current, as for other constructs containing G466A. A Western blot of this double mutant showed roughly equivalent levels of protein synthesis as obtained in other constructs and a pattern of immature glycosylation more similar to G466A than to wild-type channels (Fig. 10 C). These results support the idea that neither function nor the glycosylation defect caused by the G466A mutation can be rescued by relief of a potential steric clash between Ala466 and Met440.

We further tested whether the double mutant G466A/V467G is functional simply because of the reduction in side-chain volume at residue 467, rather than an enhancement of helical flexibility in this location. If so, then V467A might also be expected to rescue the lethal G466A. Although not as small as Gly, Ala is 38 $Å^3$ smaller than Val. The single mutant V467A is functional (Zhou et al., 2001a; Yifrach and MacKinnon, 2002). However, G466A/V467A is nonfunctional (no voltage-activated currents in eight transfected cells) and exhibits the immature glycosylation pattern found in all constructs containing G466A (Fig. 10 C). These results suggest that the flexibility of the S6 helix at position 466 (or 467) is more important for function than the sizes of the residues at these positions, whereas normal glycosylation absolutely requires a Gly residue at position 466.

DISCUSSION

The critical importance of a Gly residue at position 466 in the S6 segment of *Shaker* is evident from two experimental observations. First, tetramers containing even one subunit with the G466A mutation are nonfunctional. Second, glycosylation is strongly inhibited by G466A, even in the functional double mutant G466A/V467G. The inhibition of glycosylation in all constructs containing G466A, and the lower functional expression levels of the G466A/V467G mutant, suggest a role for Gly466 in biogenesis, perhaps due to its contribution to normal folding of the channel protein in the endoplasmic reticulum. It is not clear why the G466A mutation inhibits glycosylation of *Shaker* channels, which takes place at a distant location in the extracellular S1–S2 loop (Santacruz-Toloza et al., 1994). However, we were unable to rescue this glycosylation defect or function with either of two double mutants (M440A/G466A or G466A/V467A) specifically designed to reduce steric hindrance, indicating the relative importance of flexibility of Gly466 rather than its small size. This interpretation is supported by the fact that the G466P mutant of *Shaker* is functional but, like our functional double mutant, exhibits impaired glycosylation (Magidovich and Yifrach, 2004). These authors found that only Gly or Pro residues at this position, out of a total of 10 amino acids tested, produced functional channels. While a Pro residue is significantly larger than Gly, it is also known to introduce flexibility into α helices (see below).

It is especially striking that the open channel properties of G466A/V467G are so similar to those of WT channels, indicating that a Gly residue at position 466 is not absolutely required for a relatively normal open channel structure. Rather, the position of the Gly appears to have a more significant influence on closed–open transitions, consistent with a role as a gating hinge. As stated above, the large differences in affinity for intracellular blockers between WT and G466A/V467G channels are due almost entirely to the V467G substitution, rather than to the G466A mutation.

Gly and Pro residues in the pore-lining helices of potassium channels have been suggested to play roles in activation gating. Two well-known characteristics of these residues in proteins reinforce this proposal. First, both are prevalent at kinks in α helices, and second, they are both known to enhance flexibility of helices. Gly residues are ideally suited to provide flexibility primarily because the absence of a side chain reduces restrictions on movement (Chou and Fasman, 1974). Consistent with this idea, Gly residues are commonly found in hinges and kinks in a wide variety of proteins, for example, *lac* repressor protein (Falcon and Matthews, 1999), fungal kinesins (Grummt et al., 1998), a helix-loop-helix structure in EF hand proteins (Falke et al., 1994), rhodopsin (Palczewski et al., 2000), lac permease (Abramson et al., 2003), and heme oxygenase-1 (Schuller et al., 1999). The difference in helical propensities between Gly and Ala is especially pronounced when the residue of interest is near the middle of an α helix (Chakrabartty et al., 1991; Serrano et al., 1992), exactly the situation for the conserved Gly in the pore-lining helix of many ion channels. The enhanced flexibility induced by Gly residues in transmembrane α helices has also been demonstrated by molecular dynamics simulations (Bright et al., 2002; Bright and Sansom, 2003). Many Gly residues in kinks are highly conserved, e.g., a specific residue in the loop of 567 different EF hand proteins (Falke et al., 1994). Moreover, the residue homologous to Gly466 in *Shaker* is the most conserved residue in the S6 segments of 478 potassium and cyclic nucleotide–gated channels (Jin et al., 2002). In some potassium channels the apparent homologue of Gly466 is shifted by one position either upstream or downstream (Shealy et al., 2003), consistent with our results with a functional, downstream-shifted Gly residue. There are also examples of consecutive pairs of Gly residues at the approximate position of *Shaker*'s Gly466 in the S6 segments of calcium-activated potassium channels (Shealy et al., 2003). These Gly pairs might provide enhanced flexibility for normal activation gating of these channels. Nevertheless, the channels remain functional, although somewhat incapacitated, when both are mutated to Ala (Magidovich and Yifrach, 2004). The homologue of *Shaker*'s Gly466 residue is found in a bacterial sodium channel as well, where it may also play a role in activation gating (Zhao et al., 2004).

Although not as prevalent as Gly (Li-Smerin and Swartz, 2001), Pro residues are also found at kinks in α helices (Barlow and Thornton, 1988; MacArthur and Thornton, 1991; Von Heijne, 1991). The distortion in helical structure is largely due to a steric clash between the Cγ of the proline ring at position *i* and the carbonyl O atom of residue *i*-4. Typical kink angles due to Pro residues are ∼26° (Barlow and Thornton, 1988). Pro residues not only contribute to a disruption of secondary structure. They also increase torsional flexibility, as shown in molecular dynamics simulations (Yun et al., 1991; Tieleman et al., 2001; Bright et al., 2002; Cordes et al., 2002; Bright and Sansom, 2003), and therefore could facilitate hinge-like motion.

Although the inner helix of KcsA, homologous to the S6 segment of Kv channels, lacks Pro residues and is relatively straight, the S6 segments in most Kv channels contain a Pro-*X*-Pro (*X* = Val or Ile) motif seven residues downstream from the conserved Gly. This motif has been postulated to form a pronounced kink, in both open and closed *Shaker* channels (Holmgren et al., 1998; Del Camino et al., 2000; Del Camino and Yellen, 2001; Webster et al., 2004). Mutations of these Pro residues in Kv channels have dramatic, and sometimes lethal, consequences (Hackos et al., 2002; Yifrach and MacKinnon, 2002; Harris et al., 2003; Labro et al., 2003; Sukhareva et al., 2003). Similar to the results of our study, the nonfunctional Ala substitution for one of these Pro residues can be rescued by introducing a Pro residue in the immediate vicinity (Labro et al., 2003). Finally, introduction of either Pro or Gly residues in the pore-lining helix of an inward rectifier potassium channel has profound effects on its open probability (Jin et al., 2002), supporting a role in gating.

These experimental results all indicate the importance of Gly and Pro residues in the pore-lining helix for activation gating of potassium channels. In Kv channels, the homologues of Gly466 and the Pro-*X*-Pro regions of the S6 segment are both critical for function. This leaves an open question. Are the Gly and Pro residues in the S6 helices of Kv channels acting as static kinks or dynamic hinges (Deber and Therien, 2002)? One possibility is that *Shaker*'s Pro-Val-Pro forms a static kink and that gate opening primarily involves a hinge-like motion centered on Gly466, as originally proposed by Jiang et al. (2002b). This idea is consistent with molecular dynamics simulations of *Shaker*'s S6 segment showing anisotropic hinge-bending motions in the vicinity of Gly466 (Tieleman et al., 2001). It is also conceivable that Gly466 and the Pro-Val-Pro motif together conspire to bestow the *Shaker* S6 helix with its requisite flexibility. This possibility is also suggested by molecular

dynamics simulations of transmembrane helices that show that a Gly residue upstream of a Pro residue enhances flexibility more than the Pro residue alone (Cordes et al., 2002). Whatever conformational changes underlie activation in *Shaker*, they must be consistent with changes in ionic permeability between open and closed states (Del Camino and Yellen, 2001; Soler-Llavina et al., 2003), and by evidence that the Val residue between the two Pro residues in S6 maintains a fixed orientation, with respect to the same residue in other subunits, during activation gating (Webster et al., 2004). The final arbiter among the myriad possibilities will be solid structural information about a eukaryotic voltage-gated ion channel in both closed and open states.

APPENDIX

Analysis of Dominant Negative Suppression

We start with the null hypothesis that mutant (G466A) and WT subunits associate randomly to form five stoichiometries of tetramers:

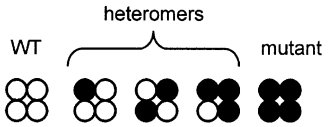

Random assembly guarantees that the distribution of tetramer compositions will be binomial. The relative proportions of WT and mutant subunits in an oocyte can be controlled approximately by the molar quantities of cRNA injected for each. Let p be the probability that a subunit is WT (p = Pr{WT}), and $1 - p$ = Pr{mutant}. Then,

$$\Pr\{\text{tetramer has } k \text{ WT subunits}\} =$$

$$B(4,k) = \binom{4}{k} p^k (1-p)^{4-k}, \quad k = 0, 1...4.$$

The data of Fig. 1, and the observation that K^+ currents are biophysically unaltered by coexpression of WT and mutant subunits, suggest that the only functional tetramers are WT homomers. We use a conditional probability in predicting the fraction of WT subunits that are functional.

$$\Pr\{\text{tetramer has } k \text{ WT subunits} | k > 0\} \equiv$$

$$S(k) = \frac{B(4,k)}{1 - B(4,0)}, \quad k = 1, 2, 3, 4.$$

The expected fraction of WT subunits in the homotetramer ($k = 4$) pool is

$$F = \frac{4S(4)}{\sum_{j=1}^{4} j \cdot S(j)}.$$

The dashed line in Fig. 1 B shows the predicted relationship between F and the fraction p of WT subunits, which is clearly inconsistent with our experimental data. To account for this discrepancy, we explore a model in which homotetramers, of either WT or mutant subunits, assemble more readily than the heteromers which produce suppression.

It is perhaps unreasonable to assume that all stoichiometries of heteromers have similar probabilities of assembling. Instead we consider the case that each mutant:WT contact confers the same additive energetic penalty for tetramer assembly (e.g., see Durkin et al., 1993). A "contact" here refers to all of the interactions between two adjacent subunits in a tetramer. The possible conformations of heteromers fall into 4 classes.

For  , all 4 arrangements have 2 mutant:WT contacts.

For  , all 4 arrangements have 2 such contacts.

For  , the 2 arrangements each have 4 such contacts.

For , all 4 arrangements have 2 such contacts.

We therefore created a modified (indicated by *) binomial distribution of stoichiometries as

$$B^*(4,k) = \frac{\eta_k B(4,k)}{\sum_{j=0}^{4} \eta_j B(4,j)},$$

with a stoichiometry-dependent penalty factor η_k defined as

$$\eta_k = \begin{cases} \exp(-2\gamma/RT) \text{ for } k = 1, 3 \\ \exp(-8\gamma/3RT) \text{ for } k = 2 \\ 1 \text{ for } k = 0, 4 \end{cases},$$

where R is the universal gas constant, T is temperature in degrees Kelvin, and γ is the energetic penalty (kcal/mol) per mutant:WT contact in a tetramer and equals zero for "no penalty."

We use $B^*(4,k)$ to compute $S^*(k)$ and the expected fraction of homotetramer WT channels (F^*), as above. We estimate the single parameter γ by a variable metric algorithm. The predicted values of F^* are shown as the solid line in Fig. 1 B.

We thank Carol Deutsch for extensive comments on the manuscript, Cathy Morris for encouraging us to test the single mutant V467G, Marilyn Woolkalis and Nancy Philp for copious biochemical guidance, and Mark Lemmon for helpful discussions about the roles of glycine residues in helical packing.

This work was supported by National Institutes of Health grant R01 AR41691.

Submitted: 15 March 2005
Accepted: 12 July 2005

REFERENCES

Abramson, J., I. Smirnova, V. Kasho, G. Verner, H.R. Kaback, and S. Iwata. 2003. Structure and mechanism of the lactose permease of *Escherichia coli*. *Science*. 301:610–615.

Armstrong, C.M. 1971. Interaction of tetraethylammonium ion derivatives with the potassium channels of giant axons. *J. Gen. Physiol.* 58:413–437.

Barlow, D.J., and J.M. Thornton. 1988. Helix geometry in proteins. *J. Mol. Biol.* 201:601–619.

Baukrowitz, T., and G. Yellen. 1996. Use-dependent blockers and exit rate of the last ion from the multi-ion pore of a K^+ channel. *Science*. 271:653–656.

Bezanilla, F. 2000. The voltage sensor in voltage dependent ion channels. *Physiol. Rev.* 80:555–592.

Bright, J.N., and M.S.P. Sansom. 2003. The flexing/twirling helix: exploring the flexibility about molecular hinges formed by proline and glycine motifs in transmembrane helices. *J. Phys. Chem. B.* 107:627–636.

Bright, J.N., I.H. Shrivastava, F.S. Cordes, and M.S.P. Sansom. 2002. Conformational dynamics of helix S6 from *Shaker* potassium channel: simulation studies. *Biopolymers*. 64:303–313.

Chakrabartty, A., J.A. Schellman, and R.L. Baldwin. 1991. Large differences in the helix propensities of alanine and glycine. *Nature*. 351:586–588.

Chou, P.Y., and G.D. Fasman. 1974. Prediction of protein conformation. *Biochemistry*. 13:222–245.

Cordes, F.S., J.N. Bright, and M.S. Sansom. 2002. Proline-induced distortions of transmembrane helices. *J. Mol. Biol.* 323:951–960.

De Souza, N.F., and S.M. Simon. 2002. Glycosylation affects the rate of traffic of the *Shaker* potassium channel through the secretory pathway. *Biochemistry*. 41:11351–11361.

Deber, C.M., and A.G. Therien. 2002. Putting the beta-breaks on membrane protein misfolding. *Nat. Struct. Biol.* 9:318–319.

Del Camino, D., M. Holmgren, Y. Liu, and G. Yellen. 2000. Blocker protection in the pore of a voltage-gated K^+ channel and its structural implications. *Nature*. 403:321–325.

Del Camino, D., and G. Yellen. 2001. Tight steric closure at the intracellular activation gate of a voltage-gated K^+ channel. *Neuron*. 32:649–656.

Ding, S., and R. Horn. 2002. Tail end of the S6 segment: role in permeation in *Shaker* potassium channels. *J. Gen. Physiol.* 120:87–97.

Ding, S., and R. Horn. 2003. Effect of S6 tail mutations on charge movement in *Shaker* potassium channels. *Biophys. J.* 84:295–305.

Domene, C., D. A. Doyle, and C. Venien-Bryan. 2005. Modeling of an ion channel in its open conformation. *Biophys. J.* 89:L01–L03.

Doyle, D.A., J.M. Cabral, R.A. Pfuetzner, A.L. Kuo, J.M. Gulbis, S.L. Cohen, B.T. Chait, and R. MacKinnon. 1998. The structure of the potassium channel: molecular basis of K^+ conduction and selectivity. *Science*. 280:69–77.

Durkin, J.T., L.L. Providence, R.E. Koeppe II, and O.S. Andersen. 1993. Energetics of heterodimer formation among gramicidin analogues with an NH_2 terminal addition or deletion. Consequences of missing a residue at the join in a channel. *J. Mol. Biol.* 231:1102–1121.

Falcon, C.M., and K.S. Matthews. 1999. Glycine insertion in the hinge region of lactose repressor protein alters DNA binding. *J. Biol. Chem.* 274:30849–30857.

Falke, J.J., S.K. Drake, A.L. Hazard, and O.B. Peersen. 1994. Molecular tuning of ion binding to calcium signaling proteins. *Q. Rev. Biophys.* 27:219–290.

Flynn, G.E., and W.N. Zagotta. 2001. Conformational changes in S6 coupled to the opening of cyclic-nucleotide gated channels. *Neuron*. 30:689–698.

Grummt, M., G. Woehlke, U. Henningsen, S. Fuchs, M. Schleicher, and M. Schliwa. 1998. Importance of a flexible hinge near the motor domain in kinesin-driven motility. *EMBO J.* 17:5536–5542.

Hackos, D.H., T.H. Chang, and K.J. Swartz. 2002. Scanning the intracellular S6 activation gate in the *Shaker* K^+ channel. *J. Gen. Physiol.* 119:521–531.

Harris, T., A.R. Graber, and M. Covarrubias. 2003. Allosteric modulation of a neuronal K^+ channel by 1-alkanols is linked to a key residue in the activation gate. *Am. J. Physiol. Cell Physiol.* 285: C788–C796.

Holmgren, M., K.S. Shin, and G. Yellen. 1998. The activation gate of a voltage-gated K^+ channel can be trapped in the open state by an intersubunit metal bridge. *Neuron*. 21:617–621.

Hoshi, T., W.N. Zagotta, and R.W. Aldrich. 1990. Biophysical and molecular mechanisms of *Shaker* potassium channel inactivation. *Science*. 250:533–538.

Javadpour, M.M., M. Eilers, M. Groesbeek, and S.O. Smith. 1999. Helix packing in polytopic membrane proteins: role of glycine in transmembrane helix association. *Biophys. J.* 77:1609–1618.

Jiang, Y., A. Lee, J.Y. Chen, M. Cadene, B.T. Chait, and R. MacKinnon. 2002a. Crystal structure and mechanism of a calcium-gated potassium channel. *Nature*. 417:515–522.

Jiang, Y., A. Lee, J.Y. Chen, M. Cadene, B.T. Chait, and R. MacKinnon. 2002b. The open pore conformation of potassium channels. *Nature*. 417:523–526.

Jiang, Y., A. Lee, J.Y. Chen, V. Ruta, M. Cadene, B.T. Chait, and R. MacKinnon. 2003. X-ray structure of a voltage-dependent K^+ channel. *Nature*. 423:33–41.

Jin, T., L. Peng, T. Mirshahi, T. Rohacs, K.W. Chan, R. Sanchez, and D.E. Logothetis. 2002. The $\beta\gamma$ subunits of G proteins gate a K^+ channel by pivoted bending of a transmembrane segment. *Mol. Cell.* 10:469–481.

Johnson, J.P., Jr., and W.N. Zagotta. 2001. Rotational movement during cyclic nucleotide-gated channel opening. *Nature*. 412: 917–921.

Kelly, B.L., and A. Gross. 2003. Potassium channel gating observed with site-directed mass tagging. *Nat. Struct. Biol.* 10:280–284.

Kiss, L., and S.J. Korn. 1998. Modulation of C-type inactivation by K^+ at the potassium channel selectivity filter. *Biophys. J.* 74:1840–1849.

Kiss, L., J. LoTurco, and S.J. Korn. 1999. Contribution of the selectivity filter to inactivation in potassium channels. *Biophys. J.* 76: 253–263.

Kitaguchi, T., M. Sukhareva, and K.J. Swartz. 2004. Stabilizing the closed S6 gate in the Shaker K_v channel through modification of a hydrophobic seal. *J. Gen. Physiol.* 124:319–332.

Kuo, A., J.M. Gulbis, J.F. Antcliff, T. Rahman, E.D. Lowe, J. Zimmer, J. Cuthbertson, F.M. Ashcroft, T. Ezaki, and D.A. Doyle. 2003. Crystal structure of the potassium channel KirBac1.1 in the closed state. *Science*. 300:1922–1926.

Labro, A.J., A.L. Raes, I. Bellens, N. Ottschytsch, and D.J. Snyders. 2003. Gating of *Shaker*-type channels requires the flexibility of S6 caused by prolines. *J. Biol. Chem.* 278:50724–50731.

Lemmon, M.A., and D.M. Engelman. 1994. Specificty and promiscuity in membrane helix interactions. *Q. Rev. Biophys.* 27:157–218.

Li-Smerin, Y., and K.J. Swartz. 2001. Helical structure of the COOH terminus of S3 and its contribution to the gating modifier toxin receptor in voltage-gated ion channels. *J. Gen. Physiol.* 117:205–217.

Li, S.C., and C.M. Deber. 1992. Glycine and beta-branched residues support and modulate peptide helicity in membrane environ-

ments. *FEBS Lett.* 311:217–220.

Liu, Y.S.A., P. Sompornpisut, and E. Perozo. 2001. Structure of the KcsA channel intracellular gate in the open state. *Nat. Struct. Biol.* 8:883–887.

MacArthur, M.W., and J.M. Thornton. 1991. Influence of proline residues on protein conformation. *J. Mol. Biol.* 218:397–412.

Magidovich, E., and O. Yifrach. 2004. Conserved gating hinge in ligand- and voltage-dependent K^+ channels. *Biochemistry.* 43: 13242–13247.

Neher, E., and C.F. Stevens. 1977. Conductance fluctuations and ionic pores in membranes. *Annu. Rev. Biophys. Bioeng.* 6:345–381.

O'Neil, K.T., and W.F. DeGrado. 1990. A thermodynamic scale for the helix-forming tendencies of the commonly occurring amino acids. *Science.* 250:646–651.

Palczewski, K., T. Kumasaka, T. Hori, C.A. Behnke, H. Motoshima, B.A. Fox, I. Le Trong, D.C. Teller, T. Okada, R.E. Stenkamp, et al. 2000. Crystal structure of rhodopsin: a G protein-coupled receptor. *Science.* 289:739–745.

Papazian, D.M., X.M. Shao, S.-A. Seoh, A.F. Mock, Y. Huang, and D.H. Wainstock. 1995. Electrostatic interactions of S4 voltage sensor in *Shaker* K^+ channel. *Neuron.* 14:1293–1301.

Perozo, E., D.M. Cortes, and L.G. Cuello. 1999. Structural rearrangements underlying K^+-channel activation gating. *Science.* 285:73–78.

Russ, W.P., and D.M. Engelman. 2000. The GxxxG motif: a framework for transmembrane helix-helix association. *J. Mol. Biol.* 296: 911–919.

Santacruz-Toloza, L., Y. Huang, S.A. John, and D.M. Papazian. 1994. Glycosylation of *Shaker* potassium channel protein in insect cell culture and in *Xenopus* oocytes. *Biochemistry.* 33:5607–5613.

Schuller, D.J., A. Wilks, P.R. Ortiz de Montellano, and T.L. Poulos. 1999. Crystal structure of human heme oxygenase-1. *Nat. Struct. Biol.* 6:860–867.

Serrano, L., J.-L. Neira, J. Sancho, and A.R. Fersht. 1992. Effect of alanine versus glycine in α-helices on protein stability. *Nature.* 356:453–455.

Shealy, R.T., A.D. Murphy, R. Ramarathnam, E. Jakobsson, and S. Subramaniam. 2003. Sequence-function analysis of the K^+-selective family of ion channels using a comprehensive alignment and the KcsA structure. *Biophys. J.* 84:2929–2942.

Soler-Llavina, G.J., M. Holmgren, and K.J. Swartz. 2003. Defining the conductance of the closed state in a voltage-gated K^+ channel. *Neuron.* 38:61–67.

Spassova, M., and Z. Lu. 1998. Coupled ion movement underlies rectification in an inward-rectifier K^+ channel. *J. Gen. Physiol.* 112:211–221.

Starkus, J.G., L. Kuschel, M.D. Rayner, and S.H. Heinemann. 1997. Ion conduction through C-type inactivated *Shaker* channels. *J. Gen. Physiol.* 110:539–550.

Sukhareva, M., D.H. Hackos, and K. Swartz. 2003. Constitutive activation of the Shaker Kv channel. *J. Gen. Physiol.* 122:541–556.

Tieleman, D.P., I.H. Shrivastava, M.R. Ulmschneider, and M.S. Sansom. 2001. Proline-induced hinges in transmembrane helices: possible roles in ion channel gating. *Proteins.* 44:63–72.

Tikhonov, D.B., and B.S. Zhorov. 2004. In silico activation of KcsA K^+ channel by lateral forces applied to the C-termini of inner helices. *Biophys. J.* 87:1526–1536.

Von Heijne, G. 1991. Proline kinks in transmembrane α-helices. *J. Mol. Biol.* 218:499–503.

Webster, S.M., D. Del Camino, J.P. Dekker, and G. Yellen. 2004. Intracellular gate opening in Shaker K^+ channels defined by high-affinity metal bridges. *Nature.* 428:864–868.

Yarov-Yarovoy, V., J.C. McPhee, D. Idsvoog, C. Pate, T. Scheuer, and W.A. Catterall. 2002. Role of amino acid residues in transmembrane segments IS6 and IIS6 of the Na^+ channel α subunit in voltage-dependent gating and drug block. *J. Biol. Chem.* 277: 35393–35401.

Yellen, G. 1998. The moving parts of voltage-gated ion channels. *Q. Rev. Biophys.* 31:239–295.

Yellen, G. 2002. The voltage-gated potassium channels and their relatives. *Nature.* 419:35–42.

Yifrach, O., and R. MacKinnon. 2002. Energetics of pore opening in a voltage-gated K^+ channel. *Cell.* 111:231–239.

Yun, R.H., A. Anderson, and J. Hermans. 1991. Proline in α-helix: stability and conformation studied by dynamics simulation. *Proteins Struct. Funct. Genet.* 10:219–228.

Zagotta, W.N., T. Hoshi, and R.W. Aldrich. 1990. Restoration of inactivation in mutants of *Shaker* potassium channels by a peptide derived from ShB. *Science.* 250:568–571.

Zhao, Y., V. Yarov-Yarovoy, T. Scheuer, and W.A. Catterall. 2004. A gating hinge in Na^+ channels: a molecular switch for electrical signalling. *Neuron.* 41:859–865.

Zhou, M., J.H. Morais-Cabral, S. Mann, and R. MacKinnon. 2001a. Potassium channel receptor site for the inactivation gate and quaternary amine inhibitors. *Nature.* 411:657–661.

Zhou, Y., J.H. Morais-Cabral, A. Kaufman, and R. MacKinnon. 2001b. Chemistry of ion coordination and hydration revealed by a K^+ channel-Fab complex at 2.0 Å resolution. *Nature.* 414:43–48.